Available online at www.sciencedirect.com

SCIENCE DIRECT

Journal of Organometallic Chemistry 663 (2002) 227–234

Journal of Organometallic Chemistry

www.elsevier.com/locate/jorganchem

Carbonyl substitution chemistry of neutral and cationic triruthenium cluster complexes derived from 1,1-dimethylhydrazine. Incorporation of two and three phosphane ligands

Javier A. Cabeza[a,*], Ignacio del Río[a], Santiago García-Granda[b], Lorena Martínez-Méndez[a], Víctor Riera[a]

[a] *Departamento de Química Orgánica e Inorgánica, Instituto de Química Organometálica 'Enrique Moles', Facultad de Quimica, Universidad de Oviedo-CSIC, E-33071 Oviedo, Spain*

[b] *Departamento de Química-Física y Analítica, Universidad de Oviedo, E-33071 Oviedo, Spain*

Received 19 June 2002; accepted 26 July 2002

Dedicated to Professor Pascual Royo, an outstanding organometallic chemist, on the occasion of his 65th birthday

---

Abstract

The reactivity of the neutral triruthenium carbonyl cluster $[Ru_3(\mu\text{-}H)(\mu_3\text{-}HNNMe_2)(CO)_9]$ (**1**) and its protonated derivative $[Ru_3(\mu\text{-}H)_2(\mu_3\text{-}HNNMe_2)(CO)_9][BF_4]$ (**2**), both containing a face-capping five-electron donor 1,1-dimethylhydrazido ligand, with an excess of triphenylphosphane and with bis(diphenylphosphanyl)methane (dppm) has been studied. With PPh_3, compound **1** gives initially two independent monosubstituted isomeric intermediates that react with more ligand to afford $[Ru_3(\mu\text{-}H)_2(\mu_3\text{-}HNNMe_2)(C_6H_4PPh_2)(PPh_3)(CO)_6]$ as the final product. This complex contains terminal and cyclometalated triphenylphosphane ligands attached to the same Ru atoms as the NMe_2 and the NH fragments, respectively. The reaction of complex **2** with PPh_3 affords, sequentially, the cationic mono-, di- and trisubstituted derivatives $[Ru_3(\mu\text{-}H)_2(\mu_3\text{-}HNNMe_2)(PPh_3)_n(CO)_{9-n}][BF_4]$ ($n = 1$–3). Unusually, the di- and trisubstituted complexes contain one PPh_3 ligand in an axial position. The reaction of complex **1** with dppm gives the disubstituted derivative $[Ru_3(\mu\text{-}H)(\mu_3\text{-}HNNMe_2)(\mu\text{-dppm})(CO)_7]$, which contains the P atoms attached to the same Ru atoms as the NH fragment. Protonation of this complex with $[HOEt_2][BF_4]$ gives the cationic derivative $[Ru_3(\mu\text{-}H)_2(\mu_3\text{-}HNNMe_2)(\mu\text{-dppm})(CO)_7][BF_4]$. However, the reaction of complex **2** with dppm leads to an inseparable mixture of products. Many of these results contrast with those previously known for carbonyl substitution reactions on triruthenium clusters isostructural with compounds **1** and **2** but containing other face-capping five-electron donor ligands. The hardness of the donor atoms of the bridging ligand is presented as an important factor in relation to the observed regioselectivity.

Keywords: Ruthenium; Ruthenium clusters; Carbonyl substitution reactions; 1,1-Dimethylhydrazine; Crystal structures

---

1. Introduction

The substitution of a phosphane ligand for a CO ligand in carbonyl metal clusters is a common reaction [1]. However, despite the great number of such reactions reported to date, for a given cluster complex, the precise coordination site that is prone to undergo a carbonyl substitution cannot be predicted in many occasions.

In this field, we have previously reported the carbonyl substitution chemistry of the cluster complexes $[Ru_3(\mu\text{-}H)(\mu_3\text{-}HNCONMe_2)(CO)_9]$ (**A**) [2], $[Ru_3(\mu\text{-}H)(\mu_3\text{-ampy})(CO)_9]$ (**B**; Hampy = 2-amino-6-methylpyridine) [3–7] and the protonated derivative $[Ru_3(\mu\text{-}H)_2(\mu_3\text{-ampy})(CO)_9][BF_4]$ (**C**) [3–7]. These compounds contain face-capping five-electron donor ligands attached to the three ruthenium atoms through two heteroatoms. Without exception, on complexes **A**–**C**, the first substitution process takes place at an equatorial site of a ruthenium atom attached to both the hydride and the amido fragment of the bridging ligand. This regioselectivity

---

* Corresponding author. Tel.: +34-985-103501; fax: +34-985-103446

E-mail address: jac@sauron.quimica.uniovi.es (J.A. Cabeza).

PII: S0022-328X(02)01777-1

has been associated with the *cis*-labilizing effect provoked by the hardness of both the amido and hydride ligands [3,4].

In 1990, Süss-Fink and coworkers published the synthesis of several triruthenium carbonyl derivatives of the type $[Ru_3(\mu\text{-}H)(\mu_3\text{-}HNNR^1R^2)(CO)_9]$ by treatment of $[Ru_3(CO)_{12}]$ with hydrazines [8]. These compounds are isostructural with complexes **A** and **B**, but their face-capping five-electron donor ligands are hydrazido fragments, which are harder than ureato and 2-amidopyridine fragments. This fact prompted us to study the CO substitution chemistry of $[Ru_3(\mu\text{-}H)(\mu_3\text{-}HNNMe_2)(CO)_9]$ (**1**) and its protonated derivative $[Ru_3(\mu\text{-}H)_2(\mu_3\text{-}HNNMe_2)(CO)_9][BF_4]$ (**2**) (Scheme 1), in order to compare it with that known for the derivatives **A**–**C** and to draw some conclusions on the influence of ligand electronic factors (hardness) in the regioselectivity of CO substitution reactions by phosphane ligands on carbonyl cluster complexes.

We have already reported the reactions of complexes **1** and **2** with one equivalent of triphenylphosphane [9], showing that the preferred site for CO substitution in these compounds is an equatorial site on the Ru atom attached to the NMe_2 fragment and not to the amido fragment, as occurred with compounds **A**–**C**. We now report the reactions of the hydrazido clusters **1** and **2** with an excess of triphenylphosphane and with bis(diphenylphosphanyl)methane (dppm), showing that the hardness of the bridging ligand donor atoms along with the position and the nature of the phosphane ligands already present in the complexes are the main factors governing the regioselectivity of successive CO substitution processes on these carbonyl clusters.

2. Results

2.1. Reactions with triphenylphosphane

The compound $[Ru_3(\mu\text{-}H)(\mu_3\text{-}HNNMe_2)(CO)_9]$ (**1**) reacted with at least two equivalents of PPh_3 in THF at reflux temperature to give $[Ru_3(\mu\text{-}H)_2(\mu_3\text{-}HNNMe_2)(C_6H_4PPh_2)(PPh_3)(CO)_6]$ (**4**) as the final product (Scheme 2). IR monitoring of the reaction showed the presence of the isomeric monosubstituted derivatives $[Ru_3(\mu\text{-}H)_2(\mu_3\text{-}HNNMe_2)(PPh_3)(CO)_8]$ (**3a** and **3b**) in the initial stages of the reaction, but both were converted into complex **4** as the reaction progressed. A mixture of **3a** and **3b** was isolated from the reaction of complex **1** with one equivalent of PPh_3 [9].

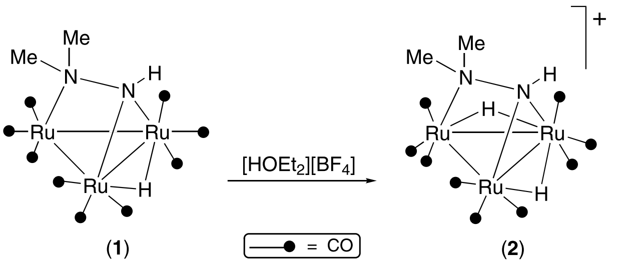

Scheme 1.

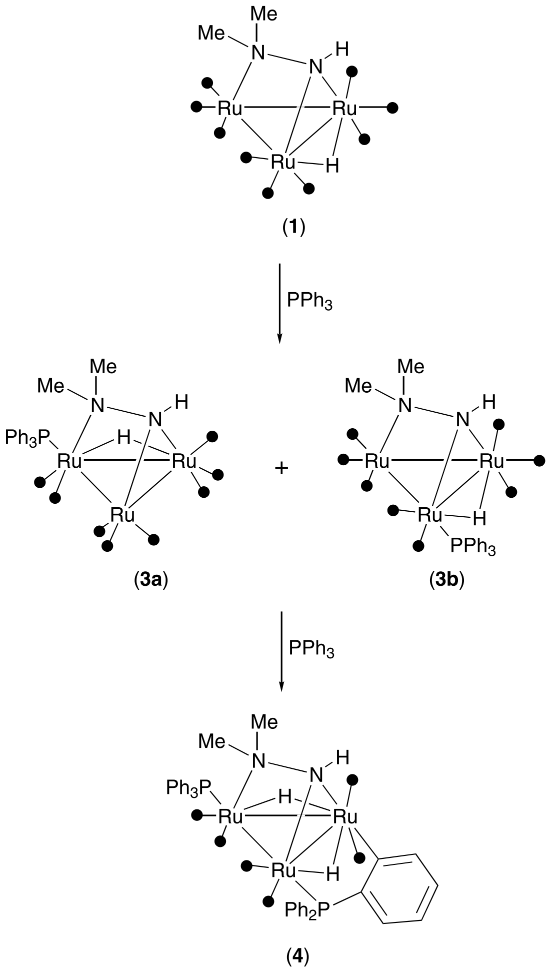

Scheme 2.

The structure proposed for complex **4** in Scheme 2 is mainly based on NMR data and on the fact that both **3a** and **3b** gave **4** when treated with PPh_3. Its composition was indicated by its microanalysis and FAB MS data. Its ^1H-NMR spectrum (Table 1) shows four C–*H* resonances clearly separated from those of the normal phenyl rings, indicating orthometalation. The observation of two hydride resonances also supported the orthometalation; the fact that they are doublets with small coupling constants (12.3 and 11.3 Hz) indicated that each P atom is *cis* to a hydride [3,4,9] and that the PRu–RuP edge is not spanned by a hydride because, in such a case, that hydride would be *trans* to at least one P atom and a larger J(H–P) coupling constant would be expected [4–6]. Its $^{31}P\{^1H\}$-NMR spectrum consists of two doublets with a large J(P–P) coupling constant (51.3 Hz), in agreement with a colinear arrangement of the two P atoms with a Ru–Ru bond [4]. As suggested

Table 1
^{1}H- and ^{31}P{^{1}H}-NMR data for the new complexes [a]

Compounds	^{1}H-NMR				^{31}P{^{1}H}-NMR
	NH	Me_2	μ-H	Phosphane	
4	4.30 (d, 6.8)	2.65 (s), 2.12 (s)	−10.90 (d, 12.3), −13.37 (d, 11.3)	7.90 (t, 6.8, 1 H), 7.45 (m, 25 H), 6.93 (t, 6.8, 1 H), 6.82 (t, 6.8, 1 H), 6.66 (t, 6.8, 1 H)	27.7 (d, 51.3), 0.3 (d, 51.3)
6 [b]	4.76 (d, 7.9)	3.04 (s), 2.41 (s)	−12.33 (ddd, 3.5, 2.6, 1.2), −14.71 (ddd, 4.6, 2.6, 1.2)	7.40 (m, 30 H)	39.1 (s), 29.8 (s)
7	4.37 (d, 7.6)	2.41 (s), 2.30 (s)	−12.02 (m), −12.95 (m)	7.40 (m, 45 H)	38.5 (s), 27.1 (d, 62.3), 22.3 (d, 62.3)
8	7.06 (t, 6.9)	2.86 (s)	−12.36 (t, 8.6)	7.30 (m, 20 H), 4.88 (m, 1 H), 4.27 (m, 1 H)	11.5 (s)
9	6.88 (t, 5.5)	3.13 (s)	−12.41 (s, br), −13.72 (d, br, 38.1)	7.40 (m, 20 H), 4.17 (m, 1 H), 3.57 (m, 1 H)	7.0 (d, 37.1), 2.3 (d, 37.1)

[a] Spectra run in $CDCl_3$ at room temperature; multiplicities and coupling constants (Hz) are given in parentheses.
[b] Data extracted from the spectra of a mixture of complexes **5**, **6** and **7**.

in Scheme 2, it is the phosphane ligand attached to the same Ru atom as the NH fragment that underwent orthometalation. We feel inclined to this proposal because the hydride that spans the same Ru–Ru edge as the NH fragment is well out of the plane of the metal atoms, thus allowing the approach of a phenyl ring to the neighbouring metal atom, whereas the other hydride ligand is ca. coplanar with the metal triangle [3,4,9] (see Figs. 2 and 3 for related dihydrido complexes). Related cyclometalations of PPh_3 in trinuclear clusters have been observed before [10].

These results contrast with those previously known for the reactions of compounds **A** and **B** with two equivalents of PPh_3, which give disubstitution on the two Ru atoms spanned by the NH fragment, without cyclometalation [2,4].

The reaction of complex **2** with two equivalents of PPh_3 in THF at reflux temperature gave a ca. 1.5:1:1.5 mixture of the cationic mono-, di- and trisubstituted derivatives $[Ru_3(\mu\text{-}H)_2(\mu_3\text{-}HNNMe_2)(PPh_3)_n(CO)_{9-n}][BF_4]$ ($n = 1$ (**5**), 2 (**6**), 3 (**7**)) (Scheme 3) which could not be separated. The use of at least three equivalents of PPh_3 led to the trisubstituted derivative **7** as the final product. When the reaction of **2** with five equivalents of PPh_3 was monitored by ^{31}P{^{1}H}-NMR spectroscopy (Fig. 1), it was observed that the monosubstituted derivative **5** was rapidly formed (singlet at 27.2 ppm) and that the trisubstituted derivative **7** (singlet at 38.7 and two doublets at 25.0 and 22.5 ppm) started to appear at the same time as the disubstituted complex **6** (two singlets at 39.8 and 25.9 ppm). These data explain why complex **6** could not be isolated.

The monosubstituted compound **5** was isolated from the reaction of complex **2** with one equivalent of PPh_3 [9]. Its structure was confirmed by X-ray diffraction [9].

The structure of the trisubstituted derivative **7** has been determined by X-ray diffraction. Fig. 2 shows a view of the cationic complex. A selection of bond lengths is given in Table 2. The structure is reminiscent of that of cluster **5**, with the difference that **7** has two more PPh_3 ligands and two less CO ligands than **5**. Interestingly, one PPh_3 ligand occupies an axial position *trans* to the NH fragment, while the other two are in equatorial positions forming a nearly linear P(1)–Ru(1)–Ru(3)–P(3) arrangement. The hydride ligands H(1) and H(2) span the Ru(1)–Ru(2) and Ru(2)–Ru(3) edges, respectively, both being *trans* to CO ligands.

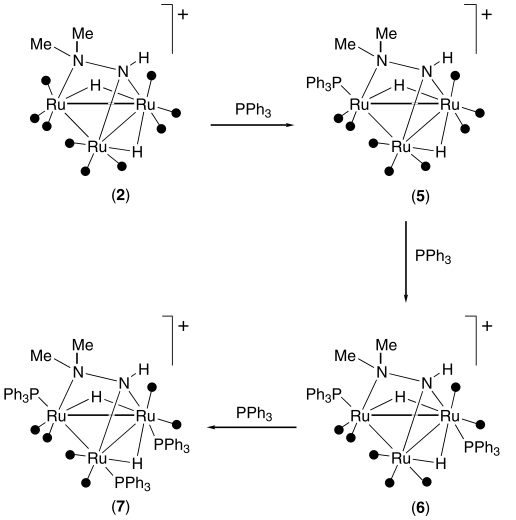

Scheme 3.

This structure clearly explains the ^{31}P{^{1}H}-NMR spectrum of this compound (Fig. 1, Table 1), which shows a singlet and two doublets with a large J(P–P) coupling constant (62.3 Hz), assignable to the axial and the two equatorial PPh_3 ligands, respectively.

Once the structures of **5** and **7** were known, that of the disubstituted derivative **6** (Scheme 3) was easily assigned from its NMR spectra (Fig. 1, Table 1) and from the

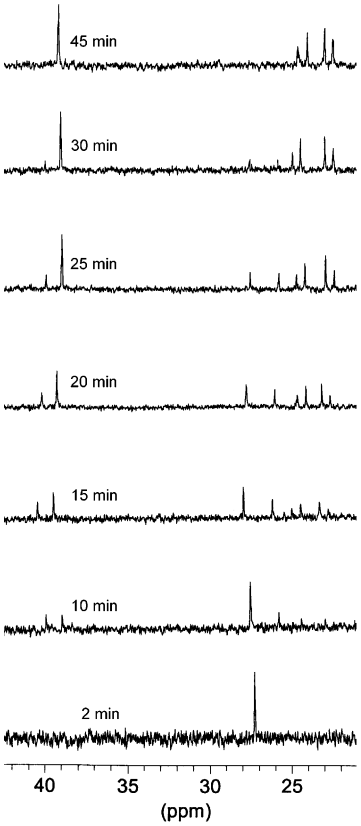

Fig. 1. $^{31}P\{^1H\}$-NMR spectra (THF, room temperature, D_2O external lock) of aliquots taken at different reaction times from the reaction of complex **2** with triphenylphosphane (1:5 mol ratio) in THF at reflux temperature.

Table 2
Selected interatomic distances (Å) in **7** and **9**

	7	**9**
Ru(1)–Ru(2)	2.8379(5)	2.7996(4)
Ru(1)–Ru(3)	2.7583(5)	2.7444(4)
Ru(2)–Ru(3)	2.9897(5)	2.9555(4)
Ru(1)–N(1)	2.135(4)	2.118(4)
Ru(2)–N(1)	2.131(4)	2.122(3)
Ru(3)–N(2)	2.207(4)	2.170(3)
Ru(1)–P(1)	2.411(1)	2.373(1)
Ru(2)–P(2)	2.376(1)	2.343(1)
Ru(3)–P(3)	2.413(1)	
Ru(1)–C(12)	1.867(5)	1.896(5)
Ru(1)–C(13)	1.904(8)	1.876(5)
Ru(2)–C(21)	1.903(6)	
Ru(2)–C(22)	1.902(5)	1.900(5)
Ru(2)–C(23)		1.903(5)
Ru(3)–C(31)	1.873(8)	1.915(5)
Ru(3)–C(32)		1.962(5)
Ru(3)–C(33)	1.858(5)	1.881(5)
Ru(1)–H(1)	1.95(6)	1.72(5)
Ru(2)–H(1)	1.70(7)	1.80(5)
Ru(2)–H(2)	1.68(6)	1.79(5)
Ru(3)–H(2)	1.80(5)	1.80(5)
N(1)–N(2)	1.473(5)	1.477(5)

fact that it is an intermediate in the formation of complex **7** from complex **5**. The multiplicity (singlets) and the chemical shifts of its two $^{31}P\{^1H\}$ resonances indicate that one PPh_3 ligand is in an equatorial position (as in **5**) and the other one is in an axial position (as in **7**).

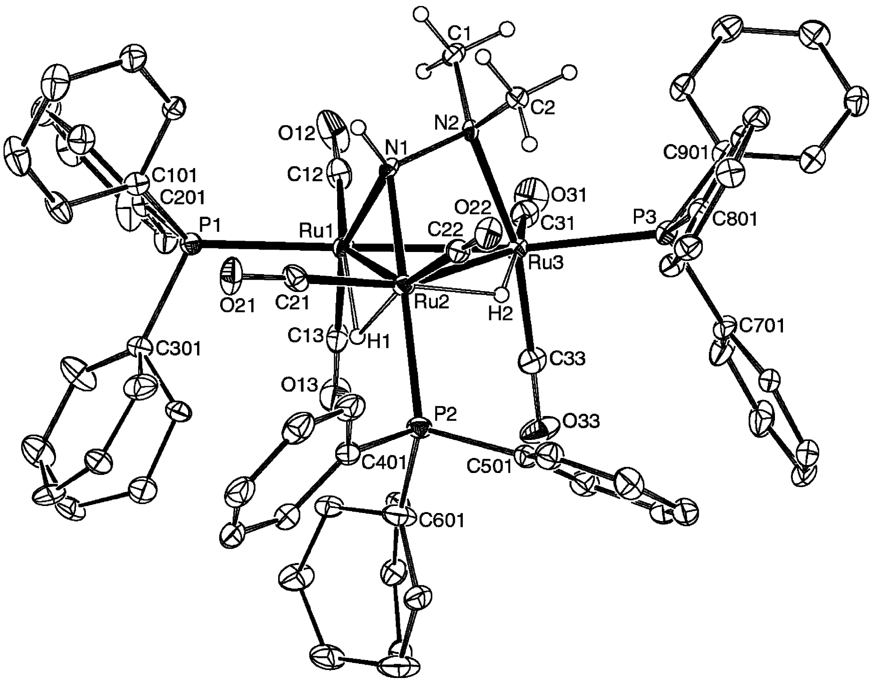

Fig. 2. Structure of the cationic part of compound **7**. Ellipsoids are drawn at the 30% probability level.

These results contrast with those previously reported for the reaction of the cationic complex [Ru$_3$(μ-H)$_2$(μ$_3$-ampy)(CO)$_9$][BF$_4$] (**C**), structurally related to **2**, with an excess of triphenylphosphane [4]. Although **C** also gives a trisubstituted complex as the final product, the stereochemistries of its mono-, di- and trisubstituted derivatives are quite different from those of the complexes derived from **2**: (a) the first substitution occurs on a Ru atom attached to the NH fragment, (b) the second one occurs on the Ru atom attached to the pyridyl fragment, in such a way that there is a linear P–Ru–Ru–P arrangement, and (c) the third one takes place on the remaining Ru atom in an equatorial site [4]. The reasons for these differences are commented below.

2.2. *Reactions with bis(diphenylphosphanyl)methane*

Treatment of compound **1** with dppm in THF at reflux temperature led to the disubstituted compound [Ru$_3$(μ-H)(μ$_3$-HNNMe$_2$)(μ-dppm)(CO)$_7$] (**8**). The structure depicted for this compound in Scheme 4 was easily deduced from its NMR spectra, which indicate C_s symmetry. Its ^{31}P{^{1}H}-NMR spectrum is just a singlet and its ^{1}H-NMR spectrum shows a singlet for both methyl groups and triplets for the hydride and N*H* resonances (Table 1). This regiochemistry is analogous to that previously observed for the reaction of the amidopyridine complex **B** with dppm [6].

Disappointingly, the reaction of the cationic compound **2** with dppm in THF at reflux temperature led to a mixture of compounds which could not be separated. Interestingly, the analogous reaction of the cationic amidopyridine complex **C** with dppm gives a disubstituted compound, which undergoes a thermal isomerization process to give a different isomer [6]. It seems probable that the different substitution regiochemistry of compound **2** as compared to that of **C**, in addition to the possibility of thermal isomerization processes, are responsible for the formation of a mixture of compounds in the reaction of **2** with dppm.

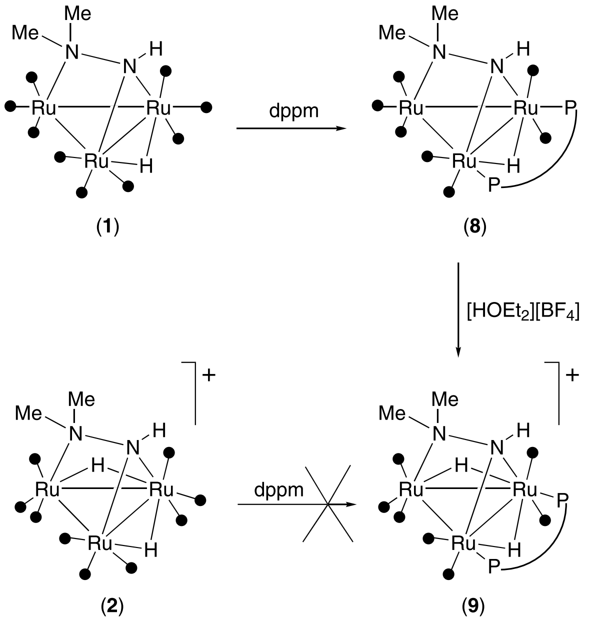

Scheme 4.

Treatment of complex **8** with tetrafluoroboric acid in dichloromethane allowed the isolation of the cationic dihydride derivative [Ru$_3$(μ-H)$_2$(μ$_3$-HNNMe$_2$)(μ-dppm)(CO)$_7$][BF$_4$] (**9**) (Scheme 4). Curiously, complex **9** is not present in the mixture obtained by treating **2** with dppm, as mentioned above. Its ^{31}P{^{1}H}-NMR spectrum shows inequivalent P atoms and its ^{1}H-NMR spectrum indicates that one of the two hydride ligands is *trans* to a P atom (J(H–P) = 38.1 Hz). This protonation reaction reminds that of the dppm derivative of complex **C** [6].

The structure depicted for this compound in Scheme 4 is supported by an X-ray diffraction study (Fig. 3, Table 2), which determined that the dppm ligand spans the same Ru–Ru edge as one of the hydrides and the NH fragment of the hydrazido ligand. The other hydride bridges one of the remaining Ru–Ru edges, being *trans* to a P atom. This structure also indicates that the atom connectivity in compound **8** is maintained after its protonation.

3. Discussion

The reactivity study reported herein, coupled with the previous one on monosubstitution reactions [9], and the comparison of these results with those known for analogous carbonyl substitution reactions on structurally related triruthenium clusters containing other face-capping ligands allow the conclusion that the regioselectivity of substitution reactions on these systems is more influenced by electronic factors associated with the ligands present in the starting complexes than by structural factors, since structurally related compounds display different reactivity.

As far as the influence of the face-capping ligand is concerned, the entering phosphane ligand ends up *cis* to a hydride ligand in an equatorial site attached to the most electrophilic metal atom, which is generally bonded to the hardest fragment of the bridging ligand. This statement is particularly applicable for the first substitution process with monophosphanes, since the observed results are in accordance with the facts that: (a) hard N-donor ligands are *cis*-labilizers [3–7]; and (b) the NMe$_2$ group is at least as hard as the NH group of the dimethylhydrazido ligand of **1** and **2** [9] and harder than the oxygen atom of the ureato ligand of **A** and the pyridyl N atom of the 2-aminopyridine ligand of **B** and **C** (both are involved in π-bonding).

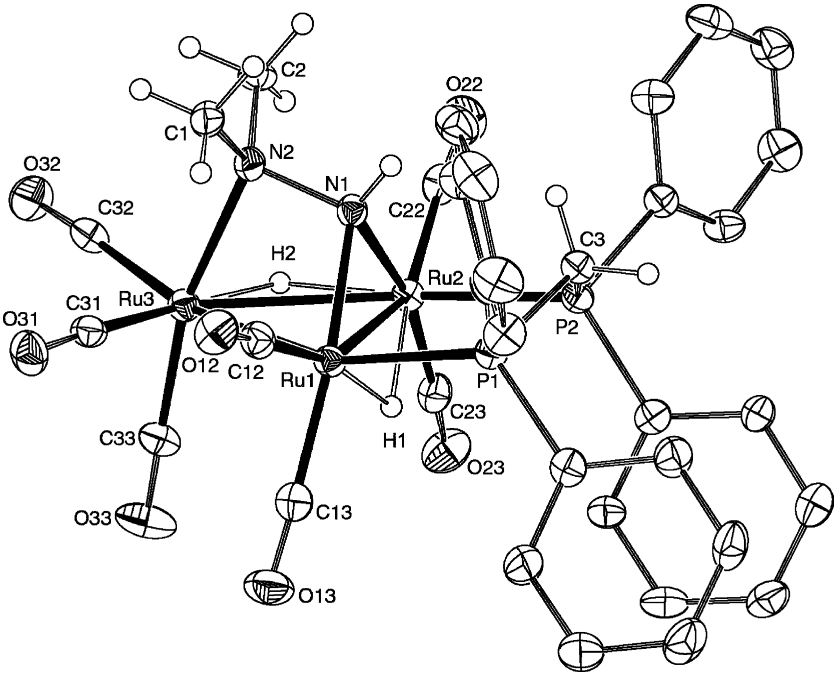

Fig. 3. Structure of the cationic part of compound **9**. Ellipsoids are drawn at the 30% probability level.

The regioselectivity observed in the di- and trisubstitution reactions by monophosphanes is more difficult to rationalise since the electrophilic effect caused by the bridging ligand is compensated to a great extent by the presence of a phosphane ligand in the complexes. It seems that these substitutions also occur on the most electrophilic metal atoms, i.e. those free of phosphane ligands, in positions *cis* to hydrides, but we have found no reasons to account for the differences observed in the derivatives of **2**, which contain an axial phosphane ligand (*trans* to a N atom), as compared with those of complex **C**, which only contain equatorial phosphanes. We are not aware of a previous example of an axial CO substitution reaction in a ligand-bridged triruthenium cluster complex.

In the case of the reactions with dppm, it seems that the bite angle of this ligand makes it particularly appropriate to span the same Ru–Ru edge as the NH fragment (at least in the neutral complexes) and that this factor is important in the regiochemistry of the reactions.

The positive charge of the cationic complexes enhances the electrophility of their metal atoms, allowing the preparation of trisubstituted products, while only disubstitutions can be obtained with neutral precursors.

For these reactions, it is important to emphasise that the stereochemistry of the final observed product should not necessarily correspond the initial substitution process (kinetic product), since rearrangements of ligand-substituted cluster carbonyls are well established, including migration of phosphane and CO ligands from one metal atom to another [3–6].

Therefore, although some aspects of the regiochemistry of these reactions have been satisfactorily explained, more work is needed, supported by theoretical studies, to completely rationalise the obtained results.

4. Experimental

4.1. General data

Solvents were dried over sodium diphenylketyl (THF, Et_2O and hydrocarbons) or CaH_2 (CH_2Cl_2, 1,2-dichloroethane) and distilled under nitrogen prior to use. The reactions were carried out under nitrogen, using Schlenk-vacuum line techniques, and were routinely monitored by solution IR spectroscopy and by spot TLC. Compounds **1** [11] and **2** [9] were prepared as described previously; all the remaining reagents were purchased from commercial suppliers. IR spectra were recorded in solution on a Perkin–Elmer Paragon 1000 FT spectrophotometer. NMR spectra (Table 1) were run on a Bruker DPX-300 instrument, using the residual solvent peak (for ^1H) or external 85% H_3PO_4 (for ^{31}P) as references. Microanalyses were obtained from the University of Oviedo Analytical Service. FAB MS were obtained from the University of Santiago de Compostela Mass Spectrometric Service; data given refer to the most abundant molecular ion isotopomer.

4.2. Synthesis of [$Ru_3(\mu$-$H)_2(\mu_3$-$HNNMe_2)(C_6H_4PPh_2)(PPh_3)(CO)_6$] (**4**)

A solution of compound **1** (50 mg, 0.081 mmol) and PPh_3 (50 mg, 0.186 mmol) in THF (20 ml) was stirred at reflux temperature for 3 h. The colour changed from yellow to orange. The solvent was removed under reduced pressure and the residue was washed with cold (−10 °C) C_6H_{14} (2 × 5 ml) and dried in vacuo to give complex **4** as an orange solid (64 mg, 73%). Anal. Found: C, 49.64; H, 3.60; N, 2.41. Calc. for $C_{44}H_{37}N_2O_7P_2Ru_3$: C, 49.43; H, 3.48; N, 2.62%. FAB MS (*m/z*): 1072 [M^+]. IR, ν(CO) (CH_2Cl_2): 2027 (m), 2008 (vs), 1976 (m), 1952 (s) cm^{-1}.

4.3. Reaction of compound **2** with two equivalents of triphenylphosphane

PPh_3 (39 mg, 0.149 mmol) was added to a solution of compound **2** (50 mg, 0.071 mmol) in THF (30 ml). The solution was stirred at reflux temperature for 45 min. The solvent was removed under reduced pressure and the oily residue was washed with C_6H_{14} (2 × 5 ml) to give a yellow solid, subsequently identified by NMR (^1H and ^{31}P) as a ca. 1.5:1:1.5 mixture of complexes **5**, **6** and **7**.

4.4. Synthesis of [$Ru_3(\mu$-$H)_2(\mu_3$-$HNNMe_2)(PPh_3)_3(CO)_6$][BF_4] (7)

PPh_3 (59 mg, 0.227 mmol) was added to a solution of compound **2** (50 mg, 0.071 mmol) in THF (30 ml). The solution was stirred at reflux temperature for 1 h. The solvent was removed under reduced pressure and the oily residue was washed with cold (−10 °C) Et_2O (2 × 6 ml) and dried in vacuo to give complex **7** as a yellow solid (66 mg, 66%). Anal. Found: C, 52.66; H, 3.95; N, 1.91. Calc. for $C_{62}H_{54}BF_4N_2O_6P_3Ru_3$: C, 52.96; H, 3.87; N, 1.99%. FAB MS (*m/z*): 1320 [$M^+ - BF_4$]. IR, ν(CO) (CH_2Cl_2): 2051 (w), 2029 (vs), 1995 (m), 1968 (s) cm^{-1}.

4.5. Synthesis of [$Ru_3(\mu$-$H)(\mu_3$-$HNNMe_2)(\mu$-$dppm)(CO)_7$] (**8**)

A solution of compound **1** (50 mg, 0.081 mmol) and dppm (34 mg, 0.089 mmol) in THF (20 ml) was stirred at reflux temperature for 30 min. The colour changed

Table 3
Crystal data and structure refinement details for compounds **7**·$C_2H_4Cl_2$ and **9**

	7·$C_2H_4Cl_2$	**9**
Empirical formula	$C_{62}H_{54}BF_4N_2O_6P_3Ru_3 \cdot C_2H_4Cl_2$	$C_{34}H_{31}BF_4N_2O_7P_2Ru_3$
Formula weight	1504.95	1031.57
Temperature (K)	120(2)	120(2)
Radiation (λ, Å)	Cu–K_α (1.54180)	Cu–K_α (1.54180)
Crystal system	Orthorhombic	Monoclinic
Space group	*Pbna*	$P2_1/n$
a (Å)	13.7325(1)	17.3035(4)
b (Å)	23.4938(2)	12.7792(3)
c (Å)	38.0230(3)	17.5747(4)
α (°)	90	90
β (°)	90	91.491(1)
γ (°)	90	90
V (Å^3)	12267.3(1)	3884.9(1)
Z	8	4
D_{calc} (g cm^{-3})	1.630	1.764
μ (mm^{-1})	7.996	10.692
F(000)	6048	2032
Crystal size (mm)	0.28 × 0.15 × 0.13	0.15 × 0.10 × 0.08
θ Limits (°)	2.32–69.65	3.54–68.47
Min/max	$0 \le h \le 16, 0 \le k \le 28, 0 \le l \le 46$	$0 \le h \le 20, 0 \le k \le 15, -21 \le l \le 21$
Reflections collected	89 372	38 687
Unique reflections	11524 ($R_{int} = 0.042$)	7132 ($R_{int} = 0.053$)
Reflections with $I > 2\sigma(I)$	9905	6120
Absorption correction	RefDelF (XABS2)	RefDelF (XABS2)
Max/min transmission	0.355/0.204	0.395/0.234
Parameters, restraints	891, 12	490, 0
Final R_1 (on *F*, $I > 2\sigma(I)$)	0.0484	0.0356
Final wR_2 (on F^2, all data)	0.1874	0.1143
Goodness-of-fit on F^2	1.067	1.051
Min/max residuals (e Å^{-3})	−1.201/2.569	−0.736/1.767

from yellow to orange. The solvent was removed under reduced pressure and the residue was washed with C_6H_{14} (2 × 5 ml) and dried in vacuo to give complex **8** as an orange solid (57 mg, 75%). Anal. Found: C, 43.39; H, 3.01; N, 2.94. Calc. for $C_{34}H_{28}N_2O_7P_2Ru_3$: C, 43.36; H, 2.99; N, 2.97%. FAB MS (*m*/*z*): 943 [M^+]. IR, *ν*(CO) (CH_2Cl_2): 2049 (s), 2032 (s), 1982 (vs), 1968 (s), 1945 (s), 1917 (m), 1891 (w) cm^{-1}.

4.6. Synthesis of $[Ru_3(\mu\text{-}H)_2(\mu_3\text{-}HNNMe_2)(\mu\text{-}dppm)(CO)_7][BF_4]$ (**9**)

A drop of a solution of tetrafluoroboric acid (54% w/w in Et_2O) was added with a Pasteur pipette to a solution of complex **8** (50 mg, 0.052 mmol) in CH_2Cl_2 (10 ml). The solvent was removed and the oily residue was dissolved in Et_2O (ca. 2 ml). Addition of C_6H_{14} (5 ml) led to the precipitation of an orange solid, which was filtered, washed with C_6H_{14} (2 × 5 ml) and dried in vacuo to give complex **9** as an orange solid (49 mg, 92%). Anal. Found: C, 39.69; H, 2.89; N, 2.71. Calc. for $C_{34}H_{28}BF_4N_2O_7P_2Ru_3$: C, 39.66; H, 2.84; N, 2.72%. FAB MS (*m*/*z*): 944 [$M^+ - BF_4$]. IR, *ν*(CO) (CH_2Cl_2): 2080 (s), 2059 (m), 2020 (s), 1012 (s), 1962 (w) cm^{-1}.

4.7. X-ray structure determinations of $\mathbf{7} \cdot C_2H_4Cl_2$ and **9**

Suitable crystals were obtained by slow diffusion of hexanes into 1,2-dichloroethane (**7**) or CH_2Cl_2 (**9**) solutions of the appropriate complexes. Diffraction data were collected on a Nonius Kappa-CCD diffractometer equipped with a 95 mm CCD camera on a κ-goniostat, using graphite-monochromated Cu–K_α radiation. Data were reduced to F_o^2 values. The structures were solved by Patterson methods with DIRDIF-96 [12] and refined with SHELX-97 [13] against F^2 of all reflections. Empirical absorption corrections were applied using XABS2 [14], with maximum and minimum transmission factors of 0.355 and 0.204, respectively, for $\mathbf{7} \cdot C_2H_4Cl_2$, and 0.395 and 0.234, respectively, for **9**. All non-H atoms were refined anisotropically. The hydride H atoms of both complexes and the hydrogen atoms H(3a), H(3b), H(10), H(303) and H(603) of $\mathbf{7} \cdot C_2H_4Cl_2$ were located in the corresponding Fourier maps, and were refined with free coordinates and thermal parameters. The hydrogen atom H(10) of complex **9** was located and refined with a fixed thermal parameter. All the remaining hydrogen atoms were geometrically calculated and refined riding on their parent atoms. Two of the nine phenyl rings of $\mathbf{7} \cdot C_2H_4Cl_2$ were found disordered over two positions, with a 50% occupancy each. For $\mathbf{7} \cdot C_2H_4Cl_2$, both the solvent molecule and the $[BF_4]^-$ anion were disordered and were treated with a mixture of constraints and restraints as described elsewhere [15]. Drawings and structure calculations were performed with PLATON [16]. The WINGX program package was used throughout the structure determinations [17]. A selection of crystal data and structure refinement details are given in Table 3.

5. Supplementary material

Complete crystallographic data for the structural analyses have been deposited with the Cambridge Crystallographic Data Centre, CCDC nos. 187603 and 187604 for compounds **7** and **9**, respectively. Copies of this information may be obtained free of charge from The Director, CCDC, 12 Union Road, Cambridge CB2 1EZ, UK (Fax: +44-1223-336033; e-mail: deposit@ccdc.cam.ac.uk or http://www.ccdc.cam.ac.uk).

Acknowledgements

Financial support from the Spanish DGESIC (grants PB98-1555 to J.A.C., and BQU2000-0219 to S.G.-G.) is gratefully acknowledged.

References

[1] For reviews on general reactivity of triruthenium carbonyl clusters, see: (a) M.I. Bruce, in: G. Wilkinson, F.G.A. Stone, E.W. Abel (Eds.), Comprehensive Organometallic Chemistry, vol. 4, Pergamon, London, UK, 1982, p. 843;
(b) M.I. Bruce, Coord. Chem. Rev. 76 (1987) 1;
(c) A.J. Deeming, in: E.W. Abel, F.G.A. Stone, G. Wilkinson, D.F. Shriver, M.I. Bruce (Eds.), Comprehensive Organometallic Chemistry II, vol. 7, Pergamon, London, UK, 1995, p. 683.

[2] J.A. Cabeza, I. del Río, V. Riera, S. García-Granda, S.B. Sanni, Organometallics 16 (1997) 3914.

[3] P.L. Andreu, J.A. Cabeza, V. Riera, C. Bois, Y. Jeannin, J. Chem. Soc. Dalton Trans. (1990) 3347.

[4] P.L. Andreu, J.A. Cabeza, M.A. Pellinghelli, V. Riera, A. Tiripicchio, Inorg. Chem. 30 (1991) 4611.

[5] P.L. Andreu, J.A. Cabeza, V. Riera, Inorg. Chim. Acta 186 (1991) 225.

[6] P.L. Andreu, J.A. Cabeza, J.L. Cuyás, V. Riera, J. Organomet. Chem. 427 (1992) 363.

[7] S. Alvarez, P. Briard, J.A. Cabeza, I. del Río, J.M. Fernández-Colinas, F. Mulla, L. Ouahab, V. Riera, Organometallics 13 (1994) 4360.

[8] T. Jemke, H. Stoeckli-Evans, G. Süss-Fink, J. Organomet. Chem. 391 (1990) 395.

[9] J.A. Cabeza, I. del Río, S. García-Granda, L. Martínez-Méndez, V. Riera, Inorg. Chim. Acta, in press.

[10] (a) C.W. Bradford, R.S. Nyholm, G.J. Gainsford, J.M. Guss, P.R. Ireland, R. Mason, Chem. Commun. (1972) 87;
(b) Y. Chi, H.F. Hsu, L.K. Liu, S.M. Peng, G.H. Lee, Organometallics 11 (1992) 1763.

[11] B. Hansert, H. Vahrenkamp, Chem. Ber. 126 (1993) 2017.

[12] P.T. Beurskens, G. Beurskens, W.P. Bosman, R. de Gelder, S. García-Granda, R.O. Gould, R. Israël, J.M.M. Smits, The DIRDIF-96 Program System, Crystallography Laboratory, University of Nijmegen, The Netherlands, 1996.

[13] G.M. Sheldrick, SHELXL-97, version 97-2, University of Göttingen, Germany, 1997.